Experimental and theoretical insights into the sequential oxidations of 3π-2spiro molecules derived from oligophenylenes: A comparative study of 1,2-b-DiSpiroFluorene-IndenoFluorene versus 1,2-b-DiSpiroFluorene(tert-butyl)4-IndenoFluorene

Frédéric Barrière, Cyril Poriel, Joëlle Rault-Berthelot

Experimental and theoretical insights into the sequential oxidations of 3π-2spiro molecules derived from oligophenylenes: a comparative study of 1,2-*b*-DiSpiroFluorene-IndenoFluorene *versus* 1,2-*b*-DiSpiroFluorene(*tert*-Butyl)$_4$-IndenoFluorene

Frédéric Barrière, Cyril Poriel, Joëlle Rault-Berthelot

Université de Rennes 1 - CNRS UMR 6226, Institut des Sciences Chimiques de Rennes,

Equipe Matière Condensée et Systèmes Electroactifs,

Campus de Beaulieu, Bat 10C, Avenue du Général Leclerc,

35042, Rennes Cedex, France

Frederic.Barriere@univ-rennes1.fr, Cyril.Poriel@univ-rennes1.fr,

Joelle.Rault-Berthelot@univ-rennes1.fr

Abstract

Cyclic voltammetry and differential pulse voltammetry have shown too distinct behaviours in the sequential oxidation processes of two closely related compounds, namely 1,2-*b*-DiSpiroFluorene-IndenoFluorene (**1,2-*b*-DSF-IF**) and 1,2-*b*-DiSpiroFluorene(*tert*-Butyl)$_4$-IndenoFluorene (**1,2-*b*-DSF(^{t}Bu)$_4$-IF**). **1,2-*b*-DSF-IF** is oxidized after a reversible one-electron transfer and a subsequent irreversible two-electron transfer. In contrast, **1,2-*b*-DSF(^{t}Bu)$_4$-IF** undergoes three well separated chemically reversible one-electron processes. Spectroelectrochemical monitoring of the gradual oxidation of the compounds points to a first oxidation centred on the indenofluorenyl core for both molecules. Consistent with the different electrochemical behaviour, the spectroelectrochemical data after the first oxidation is very different for both compounds and points to a specific electronic structure. This is further studied theoretically by DFT calculations of the molecules in their neutral, cationic and dicationic state which suggest an electronic reorganization in the dication **1,2-*b*-DSF(^{t}Bu)$_4$-IF^{2+}**.

Keywords: oligophenylene; spiro-compounds; spectroelectrochemistry; 3π-2spiro derivative; DFT calculations

1. Introduction

The design and the synthesis of highly sophisticated π-conjugated molecules and polymers have driven the development of organic electronics.[1] Particularly, one of the main challenges in organic electronics for the last two decades has been the design of efficient and stable blue light emitters for organic light-emitting diodes (OLED) applications.[2-7]

Chart 1. Examples of linear, 2π-1spiro and 3π-2spiro bridged oligophenylene derivatives used to tune electronic properties

In this context, bridged oligo- and polyphenylene derivatives are one class of materials that have recently emerged and play a key role in blue-emitting materials.[8,5,9-17] Of particular interest in bridged oligophenylene chemistry and physics for blue OLEDs are the bridged biphenyl unit (fluorene),[3,5,13,8,10-12] the bridged terphenyl unit (indenofluorene)[14,15,18-26] and the bridged tetra- and pentaphenyl units.[9,16,27,17,28,29] As the chain rigidity increases with an increasing number of bridged planar rings, a bathochromic shift of the emission wavelength signalling an extension of the π-conjugation is usually observed. That is for example, 420/425 nm for polyfluorenes, 430 nm for polyindenofluorenes and 445 nm for ladder-type poly-pentaphenylenes.[27]

In the last decade our group has introduced a new molecular concept called "3π-2spiro" compounds derived from oligophenylene possessing a unique molecular architecture constituted of one central π1-system linked *via* two shared spiro carbon atoms to two other π2-systems.[30,31,28,18,20,29,23,22,26,24] Modulation of the electronic properties of such molecular systems can be achieved through the modification and/or substitution of their different π-systems (π1-system, π2-systems or both). Some of these compounds have been used as emitting layer in organic light emitting diode (OLED) leading to violet to blue light emitting devices. [31,20,29,23,26,24]

It is well established that, up a to certain conjugation length limit, the longer the conjugation length, the smaller the HOMO-LUMO gap. This longer conjugation length translates to absorption (and emission) at lower energy and to more facile electrochemical oxidation and reduction. As three π-systems are present in 3π-2spiro molecules, the question of the precise localization and sequence of electron transfer arises because of the possible conjugation and delocalization between these different π-systems through the spiro-linkages and of the presence of two equivalent π-systems (*e.g.* fluorene moieties in **1,2-*b*-DSF-IF**). When the different π-systems constituting the 3π-2spiro molecule have drastically different conjugation lengths, the electronic properties are easily predictable, the longer π-system being oxidized more easily than the shorter one (i.e. in **DSF-LPP**[28] or in **1,2-*b*-DST-IF**[23], see structures chart 1). The situation then becomes more complicated when the different π-systems have similar HOMO-LUMO energy levels. The aim of the present work is to discuss such a model case comparing the different oxidation processes for **1,2-*b*-DSF-IF** and **1,2-*b*-DSF(^{t}Bu)$_4$-IF**, differing only from one another by the substitution with two *tert*-butyl groups on each fluorene unit (see structures chart 1). This study is based on the comparison of the anodic electrochemical behaviour of these molecules, in light of UV-visible spectroelectrochemistry experiments and theoretical calculations.

2. Experimental

2.1 Electrochemistry

All electrochemical experiments were performed under an argon atmosphere, using a Pt disk electrode (diameter 1 mm), the counter electrode was a vitreous carbon rod and the reference electrode was a silver wire in a 0.1 M $AgNO_3$ solution in CH_3CN. Ferrocene was added to the electrolyte solution at the end of a series of experiments. The ferrocene/ferrocenium (Fc/Fc^+)

couple served as the internal standard. The three electrode cell was connected to a PAR Model 273 potentiostat/galvanostat (PAR, EG&G, USA) monitored with the ECHEM Software. Activated Al_2O_3 was added to the electrolytic solution to remove excess moisture. All potentials are given versus the KCl-Saturated Calomel Electrode (SCE) that was calibrated at -0.405 V vs. Fc/Fc^+ system.

2.2. Spectroelectrochemistry

UV-vis spectroelectrochemical studies were performed using a UV/Vis/NIR CARY 5000-Varian spectrophotometer using a home-made cell, a platinum grid working electrode and two platinum wires as counter and reference electrodes. The three electrode cell was connected to a scanning potentiostat Model 362 (PAR, EG&G, USA). Activated Al_2O_3 was added to the electrolytic solution to remove excess moisture. All potentials are given vs. SCE.

2.3. Theoretical calculations

Full geometry optimization with Density functional theory (DFT)[32,33] were performed with the

hybrid Becke-3 parameter exchange[34-36] functional and the Lee-Yang-Parr non-local correlation functional[37] (B3LYP) implemented in the Gaussian 09 (Revision A.02) program suite[38] using the 6-31G* basis set[39] and the default convergence criterion implemented in the program. Compositions of molecular orbitals were calculated using the AOMix program[40,41]. The figures were generated with Gaussview 5.0.[42]

3. Results and discussion

Previous studies have established that **1,2-*b*-DSF-IF** undergoes two successive oxidation involving a first chemically reversible one-electron wave followed by a two-electron process after which electropolymerization occurs.[31,43] This is clearly shown in Fig. 1, left, where two successive oxidation waves are recorded between 0.0 and 2.5 V, the first one being reversible (inset). In contrast, the substitution of the two fluorene units by *tert*-butyl groups in **1,2-*b*-DSF(^{t}Bu)$_4$-IF**, leads to a different electrochemical behaviour (Fig.1, right) as three successive chemically reversible one-electron oxidations become electrochemically detectable before the irreversible two-electron process accompanied by an electropolymerization process.[43]

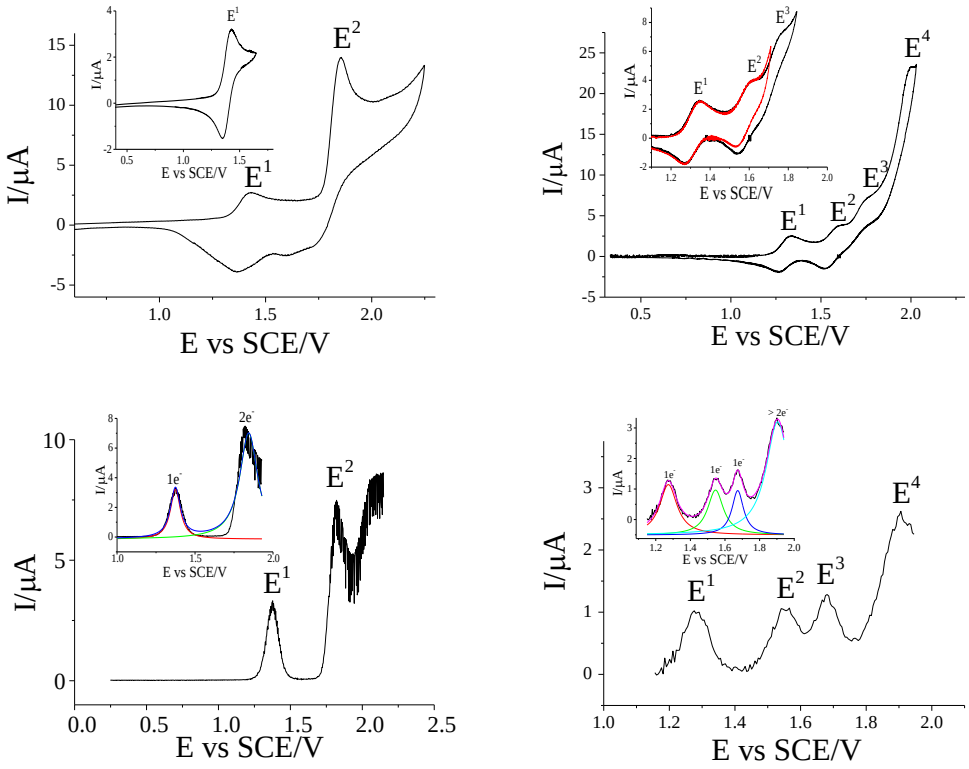

Fig. 1. Cyclic voltammetry (top) and DPV (bottom) of **1,2-*b*-DSF-IF** 2.10^{-3} M (left) and **1,2-*b*-DSF(^{t}Bu)$_4$-IF** 2.10^{-3} M (right) recorded in CH_2Cl_2 / Bu_4NPF_6 0.2 M. Insets top, zoom of the reversible waves, Inset bottom: multi-peaks fit. Platinum disk (Ø: 1 mm) working electrode. Sweep-rate : 100 mV.s^{-1} for the CV. DPV settings : Pulse Height: 25 mV, Scan-rate 50 mV.s^{-1}, Scan Increment 3 mV and Step Time 60 ms.

A better resolution and assignment of the successive oxidation processes is obtained by Differential Pulse Voltammetry (DPV) studies presented for both compounds in Fig. 1 (bottom), also showing their multi-peaks fit (inset). For **1,2-*b*-DSF-IF**, a one-electron process is followed by a two-electron process, whereas for **1,2-*b*-DSF(^{t}Bu)$_4$-IF**, three successive one-electron processes are observed before E^4.

Theoretical calculations (DFT as implemented in Gaussian 09 at the B3LYP/6-31G* level of theory) on both neutral molecules indicate that the nature of the HOMO (and of the LUMO) in **1,2-*b*-DSF-IF** and **1,2-*b*-DSF(^{t}Bu)$_4$-IF** are almost exclusively centred (>90%) on the indenofluorene core (Fig. 2).

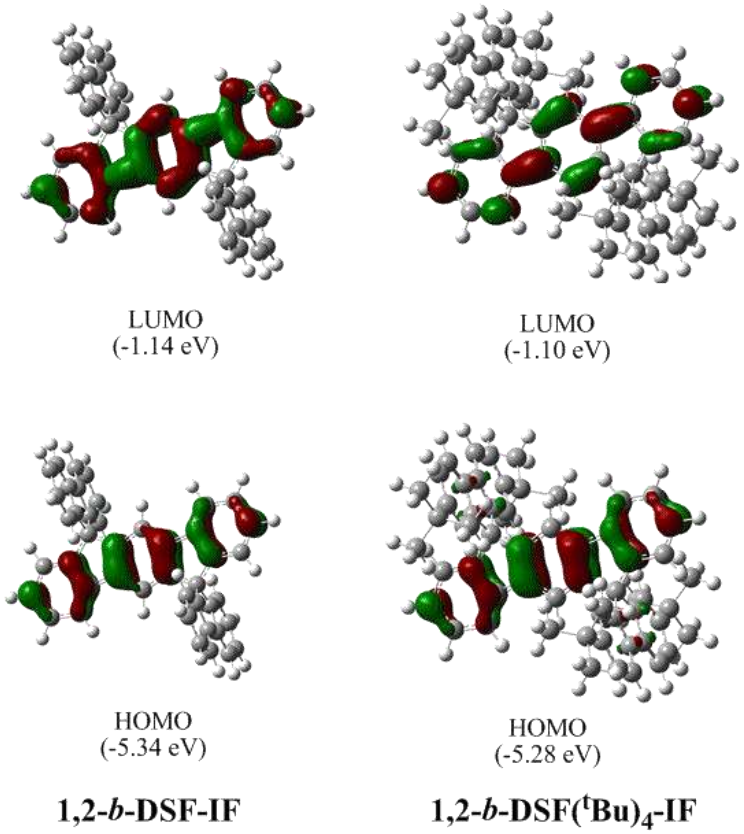

Fig. 2. Plot of the frontier molecular orbitals HOMO and LUMO of neutral **(1,2-*b*)-DSF-IF** (left) and **1,2-*b*-DSF(^{t}Bu)$_4$-IF** (right) shown with a cut-off of 0.04 [e bohr^{-3}]$^{1/2}$.

Consistent with its longer conjugation length and negligible spiro-conjugation in the HOMO, the first one-electron reversible oxidation of both molecules is then assigned to the central indenofluorene core. In addition, we note that for the two compounds the first oxidation occurs in the same potential range than that of the first oxidation of the model compound **1,2-*b*-IF** (E^1 = 1.31 V, see structure in Chart 1).[44,31] Only a weak anodic shift is observed and is readily explained by the withdrawing effect of the two fluorene units spiro-linked to the central indenofluorene core. In **1,2-*b*-DSF-IF** (E^1 = 1.43 V) the anodic shift is more pronounced than in **1,2-*b*-DSF(^{t}Bu)$_4$-IF** (E^1 = 1.33 V) and this is assigned to the levelling effect of the electron-donating *tert*-butyl substituents on the fluorene units in **1,2-*b*-DSF(^{t}Bu)$_4$-IF**. UV-visible spectra of the cation-radicals obtained along oxidation at E^1 for both molecules are presented in Fig. 3 and compared to that of **1,2-*b*-IF** radical-cation.

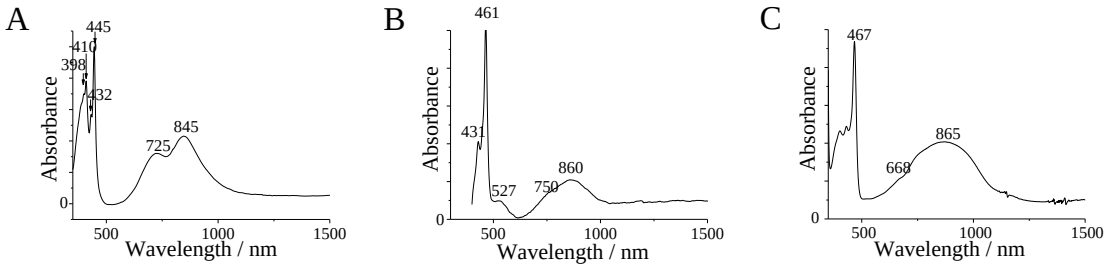

Fig. 3. UV-Vis absorption spectra recorded in CH_2Cl_2 / 0.2 M Bu_4NPF_6 of *ca.* 10^{-5} M **(1,2-*b*)-IF**$^{\cdot+}$(A), **(1,2-*b*)-DSF-IF**$^{\cdot+}$(B) and **1,2-*b*-DSF(**^{t}**Bu)**$_4$**-IF**$^{\cdot+}$ (C).

The three spectra present a similar shape with several maxima in the 350-500 nm range and two less intense and broader absorption bands around 500-1200 nm. The similarity between the UV-visible spectra and between the first oxidation potential values E^1 of **1,2-*b*-IF**$^{\cdot+}$ and those their spiro derivatives **(1,2-*b*)-DSF-IF**$^{\cdot+}$ and **1,2-*b*-DSF(**^{t}**Bu)**$_4$**-IF**$^{\cdot+}$ clearly indicates that the first oxidation is indenofluoreno-centred.

Theoretical calculations were then performed on the two 3π-2spiro radical-cations and show that the SOMO in **1,2-*b*-DSF-IF**$^{\cdot+}$ and **1,2-*b*-DSF(**^{t}**Bu)**$_4$**-IF**$^{\cdot+}$ is exclusively fluoreno-centred (Fig. 4). Hence the following oxidation should involve the fluorenyl units.

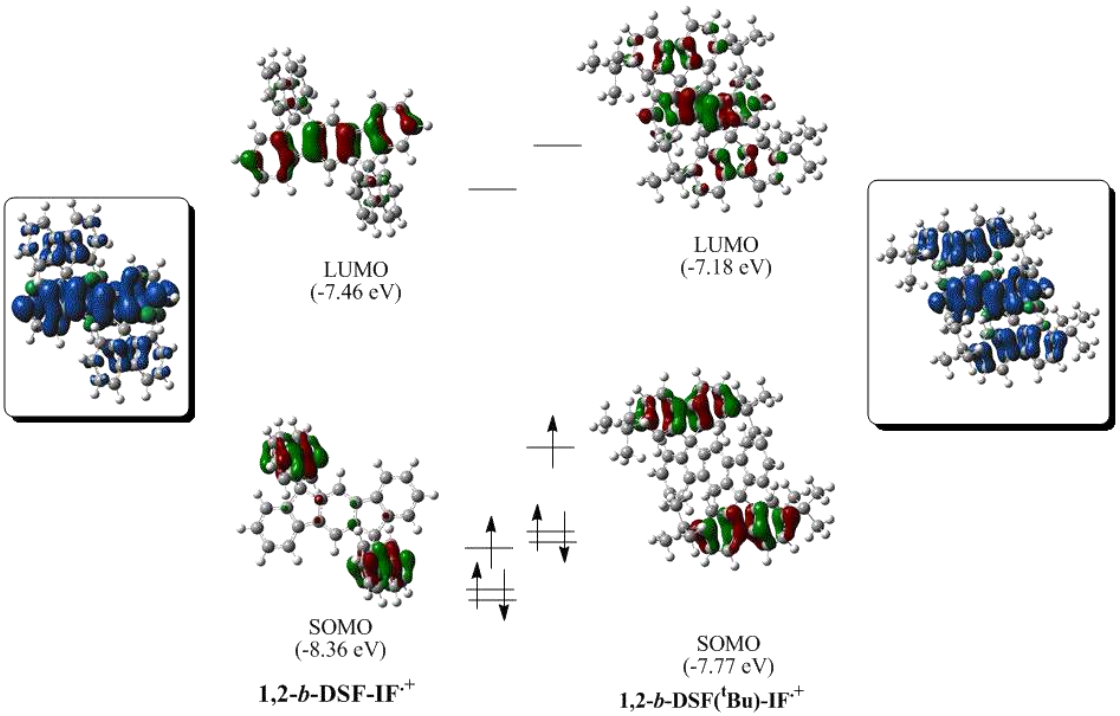

Fig. 4. Plot of the frontier molecular orbitals SOMO and LUMO of the radical cations **(1,2-*b*)-DSF-IF**$^{\cdot+}$ (left) and **1,2-*b*-DSF(**^{t}**Bu)**$_4$**-IF**$^{\cdot+}$ (right) shown with a cut-off of 0.04 [e bohr^{-3}]$^{1/2}$. Inset left and right plot of the spin density of the two radical cations with a cut-off of 0.001 e bohr^{-3}.

Theoretical calculations were finally performed on the dication of the two molecules. The triplet state of the dications has been found much more stable than the singlet state (by *ca*. 13 eV for **1,2-*b*-DSF-IF** and 12.5 eV for **1,2-*b*-DSF(^{t}Bu)$_4$-IF**). Consistently, we note that the calculated nature of the LUMO in the triplet dication (Fig.5, top) is centred exclusively on the fluorene units for both molecules. Indeed, the nature of the triplet dication LUMO indicates on which π-system a possible reduction of the dication should occur.

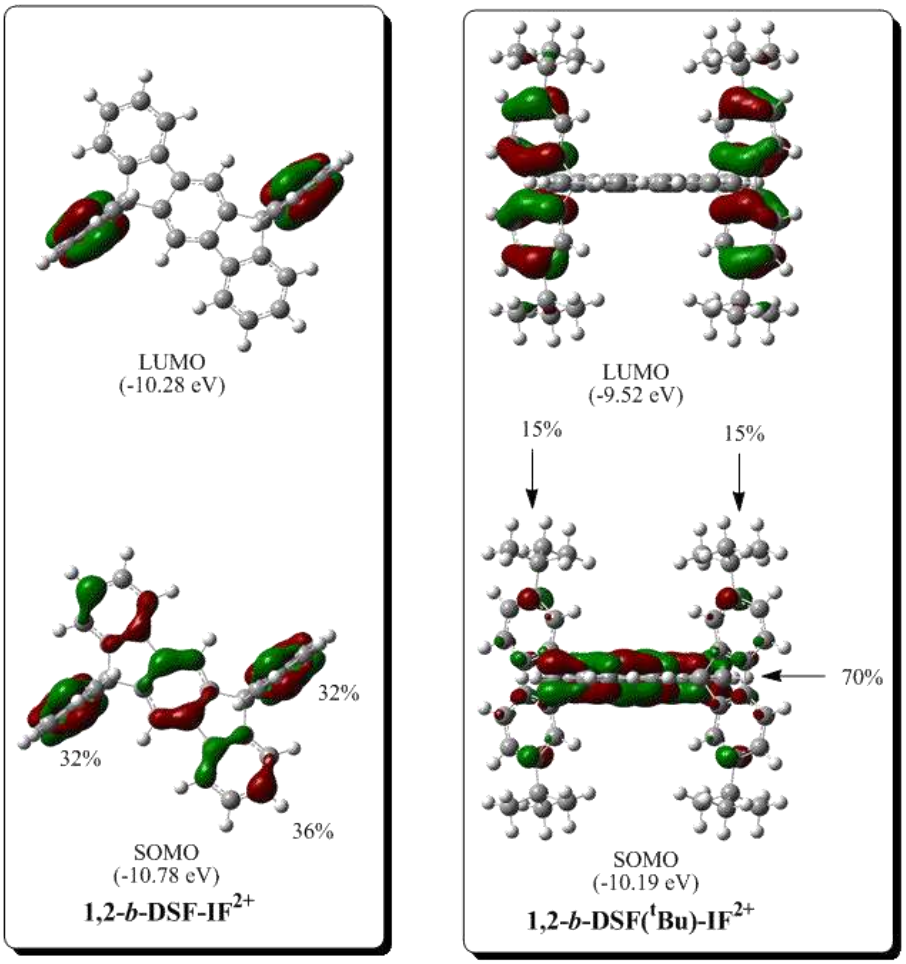

Fig. 5. Plot of the calculated nature of the frontier molecular orbitals SOMO and LUMO for the triplet state of **(1,2-*b*)-DSF-IF**$^{2+}$ (left) and **1,2-*b*-DSF(^{t}Bu)$_4$-IF**$^{2+}$ (right).

Hence, the second oxidation for both compounds is expected to occur on their fluorene units. However, CVs and DPVs recorded for both compounds appear different. Indeed, the second oxidation process involving the radical cation **1,2-*b*-DSF-IF**$^{\cdot+}$ occurs as a two-electron oxidation at E^2 (1.87 V, Cf. DPV on Fig. 1), which is slightly more anodic (+250 mV shift) than the oxidation potential of an isolated (but neutral) fluorene molecule (1.62 V).[31]

At variance, the oxidation of the radical cation **1,2-*b*-DSF(^{t}Bu)$_4$-IF**$^{\cdot+}$ occurs in two successive monoelectronic and well separated processes at 1.61 and 1.79 V, followed by a multielectronic process at 2.03 V. The oxidation at 1.61 V is anodically shifted by 190 mV compared to the (neutral) 2,7-di-*tert*-butylfluorene oxidation (1.42 V). However, one would expect the sequential oxidation of the two spiro-linked 2,7-di-*t*-butylfluorene units in **1,2-*b*-DSF(^{t}Bu)$_4$-IF**$^{\cdot+}$ to appear either as an unresolved sequential two-electron wave as observed for **1,2-*b*-DSF-IF** or as two closely spaced one-electron processes as observed for the symmetrical "2π-1spiro" derivative 9,9'-spirobifluorene (**SBF**, Chart 1) for which the oxidation involves two closely spaced one-electron processes (1.69 and 1.86 V).[45,31]

Indeed, there is a drastic difference between the anodic electrochemical behaviour of **1,2-*b*-DSF-IF** and **1,2-*b*-DSF(^{t}Bu)$_4$-IF**, the former being oxidized along two successive one and two-electron processes and the latter along three successive one-electron processes.

Interestingly, one may observe that the third oxidation of **1,2-*b*-DSF(^{t}Bu)$_4$-IF** leads to a stable triply charged species at the time scale of the cyclic voltammetry as the three first monoelectronic processes appears chemically reversible (see inset Fig. 1, top right showing the CVs recorded up to the two or three oxidation processes).

A second set of UV-visible spectroelectrochemical experiments were performed for both compounds. Evolution of the UV-spectra were recorded from E^1 (potential of the first oxidation) to higher potential values without however reaching electropolymerization for **1,2-*b*-DSF-IF** and without reaching the third electron transfer at potential higher than E^2 for **1,2-*b*-DSF(^{t}Bu)$_4$-IF**. These studies are presented in Fig. 6 and compared to the UV-visible spectrum of the model compound, **2,7-(^{t}Bu)-F**, under its radical cationic form. Consistent with the markedly different anodic electrochemistry, the two sets of UV-visible spectra also appear drastically different for **1,2-*b*-DSF-IF** in A and **1,2-*b*-DSF(^{t}Bu)$_4$-IF** in B.

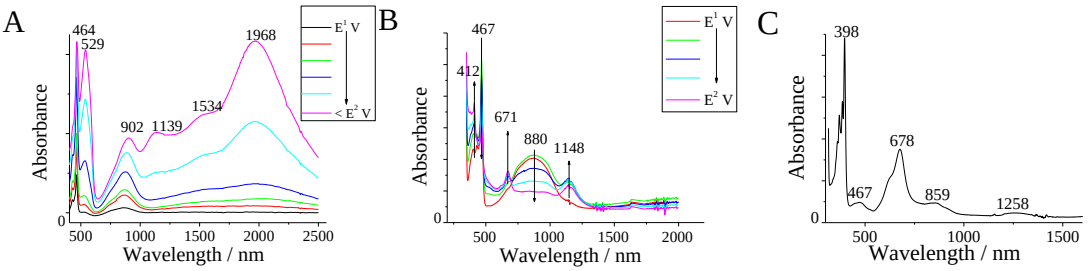

Fig. 6. UV-visible spectroscopy recorded in 10^{-5} M CH_2Cl_2 / Bu_4NPF_6 0.2 M along oxidation of **(1,2-*b*)-DSF-IF** from E^1 (first oxidation, radical-cation) to E^2 (without reaching the dication nor polymerization) (A), **(1,2-*b*)-DSF(^{t}Bu)$_4$-IF** from E^1 (first oxidation, radical-cation) to E^2 (second oxidation, dication) (B). UV-vis of **2,7-(^{t}Bu)-F**$^{\cdot+}$ radical-cation (C).

For **1,2-*b*-DSF-IF**, a gradual increase of the absorption bands detected at the radical cation state (see Fig. 3B) is observed with maxima at 464, 529, 902 and 1968 nm with however two additional bands at 1139 and 1534 nm appearing at highest potential values (Fig. 6A). This evolution signals the gradual accumulation of **1,2-*b*-DSF-IF**$^{\cdot+}$ radical-cations at the vicinity of the electrode.

During the gradual oxidation of **1,2-*b*-DSF(^{t}Bu)$_4$-IF**, a different evolution of the absorption spectra is observed. There is a clear decrease of the broad band at 880 nm, assigned to the **1,2-*b*-DSF(^{t}Bu)$_4$-IF**$^{\cdot+}$ radical-cation (Fig. 3C) at the expense of an increase of two satellite bands at 671 and 1148 nm assigned to **1,2-*b*-DSF(^{t}Bu)$_4$-IF**$^{2+}$ (Fig. 6B). We note that spectroelectrochemical studies along the first oxidation of the model compound 2,7-*tert*-butyl-fluorene, show the growth of two main bands at 398 and 678 nm (see Fig. 6C). Therefore, one can conclude that the band at 671 nm in **1,2-*b*-DSF(^{t}Bu)$_4$-IF** is indicative of a *tert*-butyl-fluorenyl radical-cation. The concomitant growth of this absorption band with the decrease of the broad band of the indenofluorenyl radical cation seems to point out a different electronic structure for this compound at the second electron transfer stage. As this hypothesis is not definitive based only on these electrochemical and spectroelectrochemical experiments, further theoretical insights were sought.

For **1,2-*b*-DSF-IF**, the SOMO of the triplet dication is delocalized evenly on the whole molecule with a fluorene-indenofluorene-fluorene ratio calculated as 32/36/32. The SOMO of **1,2-*b*-DSF(^{t}Bu)$_4$-IF** is different and its calculated nature is more localized on the indenofluorene core (ratio 15/70/15). This suggests for the latter, that the following $2^+/3^+$ process will involve the indenofluorene core and that the dication **1,2-*b*-DSF(^{t}Bu)$_4$-IF**$^{2+}$ possibly possesses two singly oxidized fluorene moieties. This supports an electronic reorganization after the second oxidation process as suggested above from the spectroelectrochemical data.

4. Conclusions

Electrochemical, spectroelectrochemical and computational chemistry experiments have shown a drastic different behaviour between **1,2-*b*-DSF-IF** and **1,2-*b*-DSF(^{t}Bu)$_4$-IF** along their successive anodic oxidations. Spectroelectrochemical studies and theoretical calculations

suggest an electronic rearrangement after the second electron transfer along **1,2-*b*-DSF(^{t}Bu)$_4$-IF** oxidation. We hypothesize that repulsion between positive charges in the bis-radical cation **1,2-*b*-DSF(^{t}Bu)$_4$-IF^{2+}** induce their localization on the 2,7-di-^{t}*Butyl*-fluorenyl units. Hence, **1,2-*b*-DSF(^{t}Bu)$_4$-IF^{2+}** might be described as a bis-radical cation with the two charges primarily localized on the π2-fluorenyl cores and with little charge on the π1-indenofluorenyl core. To the best of our knowledge such a charge rearrangement after a second electron is surprising and has only been reported once for *para*-phenylene-bridged spirobi(triarylamine) dimer containing four perpendicularly linked redox-active π-systems.[46] Interestingly, we have found a similar electrochemical behaviour for other 3π-2spiro derivatives, namely **(1,2-*b*)-DSF(Et)$_4$-IF**, **(1,2-*b*)-DSF(^{t}Bu)$_4$-IF(Br)$_2$** or different **(1,2-*b*)-DSF(phenyl-substituted)$_4$-IF** compounds.[[47]]

Acknowledgments

The authors thank the CINES (Montpellier) for the awarding of computing time.

References

[1] Special issue: π-Functional Materials; Bredas, J.-L.; Marder, S. R.; Reichmanis, E. Chem. Mater. 23 (2011) 309.
[2] K. Müllen; Scherf, U. *Organic Light-Emitting Devices: Synthesis, Properties and Applications*; Wiley-VCH Verlag GMbH & Co. KGaA: Weinheim, 2006.
[3] A. C. Grimsdale; Chan, K. L.; Martin, R. E.; Jokisz, P. G.; Holmes, A. B., Chem. Rev. 109 (2009) 897–1091.
[4] L.-H. Xie; Liang, J.; Song, J.; Yin, C.-R.; Huang, W. Curr. Org. Chem. 14 (2010) 2169.
[5] Z. Ma; Sonar, P.; Chen, Z.-K. Curr. Org. Chem. 14 (2010) 2039.
[6] A. C. Grimsdale Curr. Org. Chem. 14 (2010) 2196.
[7] T. P. I. Saragi; Spehr, T.; Siebert, A.; Fuhrmann-Lieker, T.; Salbeck, J. Chem. Rev. 107 (2007) 1011.
[8] J. Jacob; Oldridge, L.; Zhang, J.; Gaal, M.; List, E. J. W.; Grimsdale, A. C.; Müllen, K. Curr. Appl. Phys. 4 (2004) 339.
[9] J. Jacob; Sax, S.; Piok, T.; List, E. J. W.; Grimsdale, A. C.; Müllen, K. J. Am. Chem. Soc. 126 (2004) 6987.
[10] S.-R. Tseng; Li, S.-Y.; Meng, H.-F.; Yu, Y.-H.; Yang, C.-M.; Liao, H.-H.; Horng, S.-F.; Hsu, C.-S. Org. Electron. 9 (2008) 279.
[11] K.-T. Wong; Chien, Y.-Y.; Chen, R.-T.; Wang, C.-F.; Lin, Y.-T.; Chiang, H.-H.; Hsieh, P.-Y.; Wu, C.-C.; Chou, C. H.; Su, Y. O.; Lee, G.-H.; Peng, S.-M. J. Am. Chem. Soc. 124 (2002) 11576.
[12] R. Pudzich; Fuhrmann-Lieker, T.; Salbeck, J. Adv. Polym. Sci. 199 (2006) 83.
[13] M. Leclerc J. Polymer Sci.: Part A: Polymer Chem. 39 (2001) 2867.
[14] S. Setayesh; Martitzky, D.; Müllen, K. Macromolecules 33 (2000) 2016.

[15] K. H. Lee; Kim, S. O.; Kang, S.; Lee, J. Y.; Yook, K. S.; Lee, J. Y.; Yoon, S. S. Eur. J. Org. Chem. 2012 (2012) 2748–2755.
[16] J. Jacob; Sax, S.; Gaal, M.; List, E. J. W.; Grimsdale, A. C.; Müllen, K. Macromolecules 38 (2005) 9933
[17] U. Scherf J. Mater. Chem. 9 (1999) 1853.
[18] D. Thirion; Poriel, C.; Barrière, F.; Métivier, R.; Jeannin, O.; Rault-Berthelot, J. Org. Lett. 11 (2009) 4794.
[19] C. Poriel; Barrière, F.; Thirion, D.; Rault-Berthelot, J. Chem. -Eur. J. 15 (2009) 13304.
[20] N. Cocherel; Poriel, C.; Vignau, L.; Bergamini, J.-F.; Rault-Berthelot, J. Org. Lett. 12 (2010) 452.
[21] D. Thirion; Poriel, C.; Rault-Berthelot, J.; Barrière, F.; Jeannin, O. Chem. -Eur. J. 16 (2010) 13646.
[22] D. Thirion; Poriel, C.; Métivier, R.; Rault-Berthelot, J.; Barrière, F.; Jeannin, O. Chem. -Eur. J. 17 (2011) 10272.
[23] C. Poriel; Rault-Berthelot, J.; Thirion, D.; Barrière, F.; Vignau, L. Chem. -Eur. J. 17 (2011) 14031.
[24] D. Thirion; Rault-Berthelot, J.; Vignau, L.; Poriel, C. Org. Lett. 13 (2011) 4418.
[25] C. Poriel; Métivier, R.; Rault-Berthelot, J.; Thirion, D.; Barrière, F.; Jeannin, O. Chem. Commun. 47 (2011) 11703.
[26] D. Thirion; Romain, M.; Rault-Berthelot, J.; Poriel, C. J. Mater. Chem. 22 (2012) 7149.
[27] A. C. Grimsdale; Müllen, K. Macromol. Rapid Commun. 28 (2007) 1676.
[28] N. Cocherel; Poriel, C.; Rault-Berthelot, J.; Barrière, F.; Audebrand, N.; Slawin, A. M. Z.; Vignau, L. Chem. -Eur. J. 14 (2008) 11328.
[29] C. Poriel; Cocherel, N.; Rault-Berthelot, J.; Vignau, L.; Jeannin, O. Chem. -Eur. J. 17 (2011) 12631.
[30] D. Horhant; Liang, J.-J.; Virboul, M.; Poriel, C.; Alcaraz, G.; Rault-Berthelot, J. Org. Lett. 8 (2006) 257.
[31] C. Poriel; Liang, J.-J.; Rault-Berthelot, J.; Barrière, F.; Cocherel, N.; Slawin, A. M. Z.; Horhant, D.; Virboul, M.; Alcaraz, G.; Audebrand, N.; Vignau, L.; Huby, N.; Wantz, G.; Hirsch, L. Chem. -Eur. J. 13 (2007) 10055.
[32] P. Hohenberg; Kohn, W. Phys. Rev. 136 (1964) B864.
[33] R. G. Parr; Yang, W. Density-Functional Theory of Atoms and Molecules (1989) Oxford University Press: Oxford.
[34] A. D. Becke Phys. Rev. A 38 (1988) 3098.
[35] A. D. Becke J. Chem. Phys. 98 (1993) 5648 –5652.
[36] A. D. Becke J. Chem. Phys. 98 (1993) 1372.
[37] C. Lee; Yang, W.; Parr, R. G. Phys. Rev. B 37 (1988) 785.
[38] M. J. Frisch; Trucks, G. W.; Schlegel, H. B.; Scuseria, G. E.; Robb, M. A.; Cheeseman, J. R.; Scalmani, R.; Barone, G.; Mennucci, B.; Petersson, G. A.; Nakatsuji, H.; Caricato, M.; Li, X.; Hratchian, H. P.; Izmaylov, A. F.; Bloino, J.; Zheng, G.; Sonnenberg, J. L.; Hada, M.; Ehara, M.; Toyota, K.; Fukuda, R.; Hasegawa, J.; Ishida, M.; Nakajima, T.; Honda, Y.; Kitao, O.; Nakai, H.; Vreven, T.; Montgomery, J. A. J.; Peralta, J. E.; Ogliaro, F.; Bearpark, M.; Heyd, J. J.; Brother, E.; Kudin, K. N.; Staroverov, V. N.; Kobayashi, R.; Normand, J.; Raghavachari, K.; Rendell, A.; Burant, J. C.; Iyengar, S. S.; Tomasi, J.; Cossi, M.; Rega, N.; Millam, N. J.; Klene, M.; Knox, J. E.; Pomelli, C.; Ochterski, J. W.; Martin, R. L.; Morokuma, K.; Zakrzewski, V. G.; Voth, G. A.; Salvador, P.; Dannenberg, J. J.; Dapprich, S.; Daniels, A. D.; Farkas, O.; Foresman, J. B.; Ortiz, J. V.; Cioslowski, J.; Fox, D. J. Gaussian 09, version A02, Gaussian, Inc.,Wallingford, CT, 2009.

[39] P. C. Hariharan; Pople, J. A. Chem. Phys. Lett 16 (1972) 217.
[40] S. I. Gorelsky; Lever, A. B. P. J. Organomet. Chem. 635 (2001) 187.
[41] S. I. Gorelsky AOMix: Program for Molecular Orbital Analysis, http://www.sg-chem.net/, University of Ottawa, version 6.5. (2011)
[42] R. Dennington; Keith, T.; Millam, J. GaussView, Version 5, Semichem Inc., Shawnee Mission KS, 2009.
[43] C. Poriel; Rault-Berthelot, J. in preparation (2013)
[44] J. Rault-Berthelot; Poriel, C.; Justaud, F.; Barrière, F. New J. Chem. 32 (2008) 1259.
[45] J. Rault-Berthelot; Granger, M.-M.; Mattiello, L. Synth. Met. 97 (1998) 211.
[46] A. Ito; Hata, K.; Kawamoto, K.; Hirao, Y.; Tanaka, K.; Shiro, M.; Furukawa, K.; Kato, T. Chem. -Eur. J. 16 (2010) 10866.
[47] C. Poriel; Rault-Berthelot, J.; Thirion, D. J. Org. Chem. 78 (2013) 886